ELSEVIER

European Journal of Cancer 40 (2004) 1383–1396

European Journal of Cancer

www.ejconline.com

Actin-dependent tumour cell adhesion after short-term exposure to the antimetastasis ruthenium complex NAMI-A

G. Sava [a,b,*], F. Frausin [a], M. Cocchietto [b], F. Vita [c], E. Podda [c], P. Spessotto [d], A. Furlani [a], V. Scarcia [a], G. Zabucchi [c]

[a] *Department of Biomedical Sciences, University of Trieste, Via L. Giorgieri 7, 34127 Trieste, Italy*
[b] *Callerio Foundation Onlus, Trieste, Italy*
[c] *Department of Physiology and Pathology, University of Trieste, Italy*
[d] *Center of Oncological Reference, Aviano, Italy*

Received 23 April 2003; received in revised form 20 September 2003; accepted 16 January 2004
Available online 7 May 2004

Abstract

Imidazolium *trans*-imidazoledimethylsulphoxidetrachlororuthenate (NAMI-A) was tested in vitro on the pro-adhesive properties, evaluated as resistance to trypsin treatment, which is a bona fide measure of adhesion strength, of KB and HeLa carcinoma cell lines and on human polymorphonuclear neutrophils (HPMN). NAMI-A increased the pro-adhesive activity of KB cells at 0.001 mM concentration, after few minutes incubation and this effect was not influenced by the vehicle used for cell challenge, neither did it depend on NAMI-A concentration or on temperature. The same effect occurred on HeLa cells at 0.01 mM NAMI-A. This effect, detected at concentrations up to 100 times lower than those necessary to block cells at the G_2-M premitotic phase of cell cycle, or to inhibit matrix metalloproteinase release or cell invasion, was not related to ruthenium uptake by tumour cells. HeLa cells and healthy HPMN, following short exposure to 0.1 mM NAMI-A, assumed a different shape, with the extrusion of filopodia (HeLa) and of large lamellopodia (HPMN), which increased their interactions with the substrate. This effect was attributed to stabilisation, altered turnover and sensitivity to cytochalasin D of actin filaments. Provided that adhesion is associated with cell motility and invasion, these data suggest that NAMI-A may exert antimetastatic properties at concentrations lower than those observed in the lungs at the end of a conventional intraperitoneal treatment in vivo.

Keywords: Adhesion; Ruthenium; In vitro; Actin; Invasion

1. Introduction

The progression of a tumour from a benign and delimited growth to the invasive and metastatic phenotype is the major cause of poor clinical outcome in cancer patients [1]. Invasion and metastasis of tumours are highly complex and multistep processes that require a tumour cell to modulate its ability to adhere, degrade the surrounding extracellular matrix (ECM), migrate, proliferate at a secondary site and stimulate angiogenesis [1,2]. In this event, the major role is played by the interactions between tumour cells and ECM, which affect cell proliferation and survival, and their ability to migrate beyond the original location into other tissues to form metastases [3]. Cell movement is controlled by various factors, including growth and motility factors, cytokines, matrix proteins and cell-adhesion molecules [4].

Knowledge of this process has greatly increased in recent times and this has resulted in the identification of a number of molecules that are fundamental to it. The involvement of these molecules has been shown to relate not only to cell invasion but also to the survival and proliferation of the tumour cell. These molecules modulate specific steps in the invasion and metastasis processes and provide additional targets for therapies [1].

Imidazolium *trans*-imidazoledimethylsulphoxidetetrachlororuthenate (NAMI-A) is a ruthenium complex

* Corresponding author. Tel.: +39-040-569934; fax: +39-040-569-934.
E-mail address: g.sava@callerio.org (G. Sava).

0959-8049/$ - see front matter © 2004 Elsevier Ltd. All rights reserved.
doi:10.1016/j.ejca.2004.01.034

that displays antimetastatic properties, being able to reduce metastasis formation and growth in a number of mouse models [5,6]. In vitro NAMI-A may cause a transient arrest of tumour cells in the premitotic phase of the cell cycle [7], this effect being related to the intracellular concentration of the compound [8]. On in vitro cultured tumour cells, NAMI-A further reduces Matrigel® invasion [9], a phenomenon that has been associated with a reduced release of matrix metalloproteinases (MMPs) by the treated tumour cells [10] and to a direct inhibition of the same MMPs [11], and also to an increased adhesion of the treated cells [7].

On the basis of these features, and considering that the metastatic process is strongly dependent on cell motility and migration, we thought it of interest to characterise the mechanism underlying the effects of NAMI-A on cell adhesion. The study was conducted in vitro on the human carcinoma KB and HeLa cell lines, and on human neutrophils.

2. Materials and methods

2.1. Compounds and solutions

NAMI-A was synthesised and provided by Prof. E. Alessio, Department of Chemical Sciences, University of Trieste, Italy. NAMI-A was dissolved in isotonic non-pyrogenic physiological saline (PBS) and sterilised by filtration through a 0.2 μm filter. All other solutions were made in pyrogen-free distilled water for clinical use (Laboratori Diaco SpA, Trieste, Italy). The other reagents were of the highest purity available. Normal human serum (NHS) was obtained from 20 to 25 blood donors and pooled.

2.2. Zymosan preparation and opsonisation

Zymosan (10 mg/ml) was boiled in PBS for 10 min, washed once in PBS (500*g*, 10 min, room temperature) and resuspended at 10 mg/ml. 125 μg/10^6 neutrophils on zymosan particles (Sigma Chemical Co., St. Louis, MO, USA) were pelleted in the test tube in which the phagocytic assay was to be carried out. The particles were carefully resuspended in 200 μl of opsonising medium (1%, w/v, NHS diluted in PBS or IgG 1 mg/ml dissolved in PBS), incubated for 20 min at 37 °C, washed once in a small volume of PBS and finally pelleted again.

2.3. Blood neutrophils

Human neutrophils (HPMN) were isolated from the blood of healthy donors collected in a citric acid–citrate–dextrose (ACD) solution (Laboratori Diaco SpA, Trieste, Italy) and red cells were removed by dextran sedimentation (1 ml of 4.5% dextran in saline was added to 5 ml of blood). Granulocytes were separated from mononuclear cells by centrifuging the white cell-rich plasma for 20 min at 800*g* on Lymphoprep (Nycomed Pharma AS, Oslo, Norway). A 90-sc hypotonic treatment was used to remove residual erythrocytes from the granulocyte-rich pellet. The cells were washed once in PBS containing 1.2 mM Mg^{2+}, 0.5 mM Ca^{2+}, 5 mM glucose and 0.1% (w/v) bovine serum albumin (fraction V; Sigma Chemical Co., St. Louis, MO, USA) (PBS+), resuspended in the same medium, and counted electronically. The final cell suspension, as judged by differential counts, carried out on Diff-Quik-stained (Harleco, Philadelphia, PA, USA) cytospin specimens, contained >95% neutrophils, the remaining cells being eosinophils.

2.4. Tumour cell lines

An established KB cell line derived from a human epidermal carcinoma (ECACC No. 86103004) was cultured according to a standard procedure [12]. Vials of the original line were maintained in liquid N_2; cells were obtained, routinely subcultured once a week, and used for the experiments reported in the present work. The cell line was maintained in Eagle's minimum essential medium (MEM [13]) supplemented with 10% (v/v) newborn calf serum (Gibco-BRL), with 10 ml/l penicillin and streptomycin solution (Sigma) (100 U/ml penicillin G and 100 μg/ml streptomycin) and buffered with 3 mM *tris*[hydroxymethyl]methyl-2-aminoethane-sulphonic acid, 3 mM *N*,*N*-*bis*[2-hydroxy ethyl]-2-aminoethane-sulphonic acid, 3 mM *N*-2-hydroxyethyl piperazine-*N*′-2-ethane-sulphonic acid, and 3 mM Tricine (all from Sigma). The cell population doubling time was ca. 24 h. Cells from confluent monolayers were removed with 2–3 ml of trypsin solution (0.05%, w/v) (Sigma).

An established HeLa cell line (ATCC No. CCL-2) derived from human cervix adenocarcinoma was cultured according to standard procedures [14]. Subconfluent cell cultures were obtained by seeding 0.5×10^6 cells twice a week in 8 ml of complete medium in 25-cm^2 culture flasks. The medium employed was Dulbecco's modified Eagle medium (DMEM; Euroclone®, Devon, UK) supplemented with 10% (v/v) of fetal bovine serum (HyClone®, Logan, Utah, USA), 1% L-glutamine (Sigma) and 0,1% (w/v) penicillin and streptomycin solution (100 U/ml and 100 μg/ml, respectively.

For each typology of test performed, the number of cells sown, the volumes of incubation medium and the time of incubation are indicated in the corresponding sections.

2.5. Adhesion assay (resistance to trypsin treatment) on tumour cells

To evaluate any increase in cell adhesion by NAMI-A, either HeLa or KB cells were sown at a density of

3×10^4 cells/ml, in 0.2 ml/well in a 96-well plastic plate (Corning Costar Milano, Italy) and incubated at 37 °C. After 2 days (HeLa cells) or 5 days (KB cells), nutritive medium was removed and the plate washed with PBS. MEM or PBS+, with or without NAMI-A at different concentrations, were added to the wells and incubated for different times. Then, supernatant was discarded, plates were washed twice with PBS, 30 μl of (0.05%, w/v) trypsin solution was added to each well and the plates were incubated at 37 °C for 30 min. After incubation, trypsin was removed and wells washed with PBS. Non-detached cells were fixed with 200 μl of 10% (w/v) cold trichloracetic acid (TCA) at 4 °C for 1 h. After fixation, TCA was removed and wells washed with distilled water. Plates were left to dry at room temperature for few minutes before performing the sulphorhodamine B (SRB; Sigma) test.

A tumour cell-adhesion test on different substrates was performed on 96-well plates (Falcon, Franklin Lakes, NJ, USA), using the following substrates: plastic (uncoated bottom of the plates), fibronectin from human plasma, collagen IV from human placenta and poly-L-lysine 70–150 kDa (all from Sigma). Wells were coated as follows. Fibronectin and collagen IV: the original product was diluted to 20 μg/ml with sterile apyrogen water for injection (Laboratori Diaco SpA, Trieste, Italy) and added in volumes of 50 μl to the corresponding wells; poly-L-lysine: 100 μl of a 10 μg/ml solution were added to the corresponding wells. These plates were left in a humidified cell-culture chamber at 37 °C for 4 h. Before cell seeding, each plate was washed twice with sterile PBS. Then 1×10^4 cells in 200 μl of complete medium were sown in each well and cultured for 48 h. The culture medium was next removed and wells washed with PBS. Cells were then treated with 10^{-5}, 3×10^{-5} and 10^{-4} M NAMI-A for 1 h in PBS. At the end of the incubation time, NAMI-A was removed and the wells washed twice with PBS before cell adhesion was evaluated as described above.

2.5.1. Sulphorhodamine B assay

To verify the cell number in the plate wells, adherent cells in each well were dyed with a colorimetric assay based on quantification with SRB of the cell protein component [15]. SRB solution (0.4%, w/v, in 1% acetic acid) was added to the wells containing cells treated and fixed as described above, and the plates were allowed to stain for 30 min at room temperature. Unbound SRB was removed by washing twice with 1% acetic acid. Plates were air-dried, bound stain was dissolved with unbuffered 10 mM Tris base (*tris*-hydroxymethyl-aminomethane) (Sigma) at pH 10.5 and the optical density was read at 570 nm with an automatic computerised spectrophotometer (SpectraCount; Packard, USA).

The modification in cell adhesion was expressed as adhesion increment percentage in samples incubated with NAMI-A compared to control samples. Each experiment was performed with six replicates and repeated twice.

Cytochalasin D (CD) (Sigma), a potent inhibitor of actin polymerisation, and consequently, of cell adhesion on substrate, was utilised to challenge the NAMI-A-induced pro-adhesive effect on tumour cells in vitro. The 'CD test' differs from a 'cell-adhesion test on different substrates' only in having a 5-min cell preincubation with CD at the concentration of 5 μg/ml, performed immediately before treatment with NAMI-A. A first group of control wells was not pretreated with CD while a second was not treated with NAMI-A. Eight replicates of each sample and control were tested.

2.6. Adhesion assay on NAMI-A-treated human neutrophils

The adhesion of NAMI-A-treated HPMN was evaluated according to a previously reported method [16], based on the enzymatic assay of the neutrophil myeloperoxidase (MPO) activity. In brief, 5×10^6/ml HPMN, resuspended in PBS containing 0.5 mM $CaCl_2$, 1.2 mM $MgCl_2$, 5 mM glucose and 0.2% (v/v) BSA (fraction V), were either treated with NAMI-A (in the range 0.01–0.2 mM) or not. After 10-min incubation at 37 °C, 10^5 cells were sown in 96-well plates, coated with fibronectin (FN) (Sigma) (the wells were incubated with 20 μg/ml FN for 60 min at 37 °C and thoroughly washed with PBS thereafter). Plates were then incubated at 37 °C for 60 min. After incubation, 250 μl PBS were added in each well, plates were turned upside down and centrifuged for 5 min at 250*g* at room temperature to remove non-adherent cells. The extent of adhesion was evaluated by measuring the MPO content according to Menegazzi et al. [17], using tetra-methyl-benzidine (Sigma) as substrate. The number of adherent HPMN was calculated from a calibration curve obtained with a known amount of cells (from 5×10^3 to 10^5 HPMN).

2.7. Effect of integrin-blocking antibodies on the NAMI-A-induced adhesion of HPMN

The involvement of integrins in the NAMI-A-induced HPMN adhesion effect was tested by including monoclonal antibodies TS1/18 [18], TS1/22 [19] or M1/70 [20] at a concentration of 20 μg/ml in the incubation medium. All other procedures were as in the above section.

Blocking monoclonal antibodies against αL chain (TS1/22; mouse IgG1), αM chain (M1/70; rat IgG2b), and β_2 chain (TS1/18; mouse IgG1) were produced in our laboratory using the relative hybridoma purchased from ATCC. Monoclonal antibody 24 (mouse IgG1) (anti-activation domain common to the α-chains of β_2-integrins) was provided by Dr. N. Hogg (Imperial Cancer Research Fund, London, UK). Fluorescein

isothiocyanate (FITC)-conjugated antimouse IgG antibody raised in rabbit HEPES, glucose, BSA (fraction V) and paraformaldehyde were purchased from Sigma. Tumour necrosis factor-α TNF, produced by a human gene transfected in yeast (*Pichia pastoris*), was purchased from Bissendorf Biochemicals (GMBH, Hanover, Germany).

2.8. Evaluation of the activation domain of β_2-integrin on the HPMN surface

HPMN (0.5×10^6) suspended in HEPES buffer pH 7.4 (NaCl 140 mM, KCl 5 mM, $MgCl_2$ 1 mM, HEPES 5 mM, glucose 5 mM and 0.2%, v/v, BSA) were incubated for 20 min in the presence of monoclonal antibody 24, 5 μg/ml, and 0.1 mM NAMI-A, with 10 ng/ml TNF, or in the absence of stimulants. At the end of the incubation the cells were washed in PBS at room temperature and then incubated for 30 min more at room temperature with the FITC-conjugated antimouse IgG antibody and washed twice thereafter. After labelling, HPMN were fixed with 2% (w/v) paraformaldehyde for 10 min, washed and analysed by flow cytometry.

2.9. Confocal microscopic visualisation of actin filaments by FITC-conjugated phalloidin

The great affinity of phalloidin, a poisonous alkaloid obtained from *Amanita phalloides*, for actin is useful for visualising actin filaments (F-actin) inside cells [21]. About 10^5 HeLa cells were sown, in 400 μl of complete medium, on an 8-well chamber slide (Chamber Slide™ system; Lab Tek®, Nalge Nunc International, Naperville, IL, USA) and incubated for 48 h at 37 °C under 5% CO_2. Cells were then treated with PBS containing 0.1 mM NAMI-A for 1 h at 37 °C. After this challenge the cells were washed twice with PBS and fixed in 3.7% (w/v) paraformaldehyde prepared with 5.1 mM sucrose in PBS. After three washings of 1 min with PBS, cells were saturated with ammonium chloride (NH_4Cl) 50 mM for 2–5 min. After two 10-min washings with PBS, cells were permeabilised with 0.025% (w/v) saponine, and after two more washes they were treated with 4 U/ml of phalloidin (Alexa Fluor 488 phalloidin; Molecular Probes, Eugene, OR) for 20 min at 37 °C, and then finally washed again with PBS (30 min) and the chambers removed from the slides. HPMN, free in suspension, were treated either in the presence of 0.1 mM NAMI-A or in its absence, for 10 min at 37 °C. After incubation, cells were washed twice with PBS, cytocentrifuged on glass slides (Cytospin2, Shandon, Runcorn, UK) and fixed with 3.7% formaldehyde for 15 min at room temperature. Cells were then exposed to a solution containing 100 μg/ml lysophosphatidyl choline as permeabilising agent (dissolved at 25 mg/ml in absolute ethanol and diluted 250× in PBS just before use) and 4 U/ml phalloidin for 20 min at 4 °C, and washed three times (10 min) with PBS at room temperature.

Either HeLa or HPMN were then observed by confocal microscopy (DiaPHOT-200; Nikon) (confocal system MCR-1024; Bio-Rad Laboratories, Hercules, CA, USA). The 'false colour' image elaboration was done by *LaserSharp Processing* software (Bio-Rad).

2.10. Scanning electron microscopy

The effect of NAMI on the morphology of HPMN and of HeLa cells was examined by scanning electron microscopy (SEM). A total of 1×10^5 cells/ml were incubated for 60 min in PBS on Thermanox slides, either in the presence or in the absence of 0.1 mM NAMI-A. Samples were fixed in 2.5% (v/v) glutaraldehyde in 0.1 M sodium cacodylate buffer, pH 7.4, for 90 min. Cells were then washed twice in PBS and processed for SEM. In brief, coverslips were dehydrated in a graded (from 50% to 100%) ethanol series, dried in a CO_2 apparatus (Bal-Tec; EM Technology and Application, Fuerstentum, Liechtenstein), sputter-coated with gold in an Edwards S150A apparatus (Edwards High Vacuum, Crawley, West Sussex, UK), and examined on a Leica Stereoscan 430i (Leica Cambridge Ltd., Cambridge, UK) scanning electron microscope.

2.11. Phagocytosis

HPMN (2.5×10^6) resuspended in PBS containing 0.5 mM $CaCl_2$, 1.2 mM $MgCl_2$, 5 mM glucose, 0.2% BSA, either preincubated for 10 min in the presence or in the absence of 0.1 mM NAMI-A, were added to tubes containing opsonised zymosan (Sigma) 0.1 mM (312 μg). The mixture was incubated for 10 min at 37 °C. The extent of HPMN phagocytosis in the various assay conditions was monitored morphologically on cytocentrifuged specimens fixed with methanol and stained with Diff-Quik (Dade Behring, Dudingen, Switzerland) under a light microscope. At least 200 cells were observed and the number of particles/cell was counted. We defined the phagocytic index (PI) as the number of total particles ingested divided by the total number of cells observed (non-phagocytic cells included). This value takes into consideration both the percentage of phagocytic cells and the number of particles ingested per phagocytic cell.

2.12. Subcellular distribution of NAMI-A

About 3×10^6 cells were sown in an appropriate volume of complete medium in a series of 150-cm^2 flasks and cultured for 72 h for subcellular distribution. The total amount of cells employed per experiment was about 3×10^8. Cells were treated with 0.3 mM NAMI-A in complete medium for 15, 30 and 45 min at 37 °C in a bottle kept under slow and constant agitation. At the

end of incubation, cells were centrifuged at 200*g* for 10 min at 4 °C. Supernatant was removed and the pellets resuspended and washed in DMEM. Final pellets were resuspended in a relaxation buffer prepared as follows: 100 ml of sterile apyrogenic water were added to 100 mM KCl, 3 mM NaCl, 3.5 mM $MgCl_2$, 10 mM HEPES, 1 mM ATP; pH was adjusted to 7.4. Cell homogenate was obtained by cavitation in a pressure chamber (Parr Instruments Co, Moline, IL) adjusted to 350 psi nitrogen for 15 min at 0 °C with slight agitation. After cavitation, the nuclear fraction was separated from crude homogenates by centrifugation at 800*g* for 10 min at 4 °C. Three milliliters of PNS was stratified on a discontinuous saccharose gradient (AnalaR®; BDH, England) previously prepared by adding, in 13-ml cellulose acetate ultracentrifuge tubes (Beckman Instruments), 1 ml sucrose at a density of 1.22 g/ml, and 9 ml of sucrose at a density of 1.12 g/ml. The solutions were prepared by dissolving sucrose in 20 mM HEPES at pH 7.4 and controlling the density with a densitometer (DMA 45 A; Parr, Graz, Austria). Ultracentrifugation was performed overnight at 4 °C with slow acceleration and without braking (Beckman L-60 with SW40 rotor). The three main bands obtained, starting from the upper side of the tube, corresponded to cytosol, membrane and microsomal fractions, respectively. Bands were carefully collected with a syringe and the membrane and microsomal fractions were further ultracentrifuged for 1 h at 50,000*g* at 4 °C with 13 ml of 20 mM HEPES to remove residual sucrose. After protein quantitation by the Bradford test, each fraction was characterised by using specific enzymatic markers: the microsomal fraction with glucose-6-phosphatase [22] and the membrane fraction with alkaline phosphatase [23]. The ruthenium content of each fraction was quantified by atomic absorption spectroscopy (AAS).

3. Ruthenium measurement by flameless AAS

Cell specimens were dried overnight at 80 °C and then at 105 °C in Nalgene® cryovials. Cell decomposition was facilitated by the addition of a portion of tetramethyl ammonium hydroxide (25% in water) (Aldrich Chimica, Gallarate, Milano, Italy) and of milliQ water at a ratio 1:1 directly into each vial, at room temperature and under shaking (modified from [24]). Final volumes were adjusted to 1 ml with milliQ water. Ruthenium concentration was measured using a graphite-furnace atomic absorption spectrometer, model SpectrAA-220Z, supplied with the GTA 110Z powerpack and with a specific ruthenium-emission lamp (Hollow cathode lamp P/N 56-101447-00) (Varian, Mulgrave, Vic., Australia). In order to correct for possible deterioration of the graphite furnace during a daily working session, a reslope standard was measured every six samples and a full recalibration was done every 12 samples. Changes in the readings of this standard are included in the calculation of the dimeric compound concentration of the test samples. The graphite furnace was replaced when the values of two subsequent reslope readings deviated by more than 20%. The lower and higher limits of quantitation were set at the levels corresponding to the lower (20 ng Ru/ml) and higher (100 ng Ru/ml) standard concentrations, respectively. The limit of detection, 10 ng Ru/ml, was estimated according to the EURACHEM guide 'The fitness for purpose of analytical methods'. The quantification of ruthenium was carried out on 10-μl samples at 349.9 nm with an atomising temperature of 2500 °C, using argon as carrier gas at a flow rate of 3.0 l/min. Before each daily analysis session, a 5-point calibration curve was obtained using the Ruthenium Custom-Grade Standard, 998 μg/ml (Inorganic Ventures Inc., Saint Louis, MI, USA).

3.1. Statistical analysis

Data were analysed by Student's unpaired *t* test. Parallelism between regression lines was carried out with the PCS program [25]. Significance was accepted at $P < 0.05$.

4. Results

4.1. Evaluation of the pro-adhesive effect of NAMI-A on KB cells by the SRB test

The SRB test was applied to plates sown with 6×10^3–9×10^4 KB cells. The sensitivity of the SRB test is good and linear, in the range of 3–6×10^4 cells (Fig. 1 and insert), being able to detect variations of less than 5×10^3 cells per well. The SRB test was therefore used in the subsequent experiments to detect the number of cells remaining in each well after exposure to diluted trypsin.

Trypsin harvesting of cells from 96-well plates allowed a progressive appreciation of the pro-adhesive effect of 100 μM NAMI-A, depending on the duration of the challenge of KB cells with diluted trypsin. The increase in cell adhesion of 12.4% (in MEM) and of 8.3% (in PBS), observed after 15 min of trypsin exposure, reached about 30% of untreated controls, independently of the use of PBS or MEM, after 30 min, and 100% of controls, in either vehicle, after 50 min (Fig. 2). However, exposure of tumour cells to trypsin for longer than 40–50 min is inappropriate in that severe damage to cells occurs.

On the basis of these results, all subsequent experiments were done in conditions in which cells, treated with NAMI-A, were exposed to diluted trypsin for 30 min, a time that allows for good discrimination between adherent cells in groups of controls, and prevents

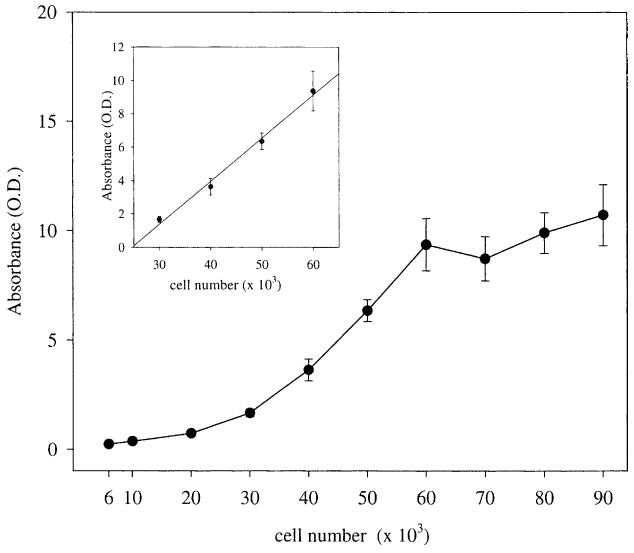

Fig. 1. Evaluation of sulphorhodamine B test sensitivity. KB cells were sown at different densities ($6–90 \times 10^3$ cells/well) on 96-well plastic plates. After 20 h the cell viability was quantified with the sulphorhodamine B assay. Insert panel shows linear regression of absorbance data of wells with $30–60 \times 10^3$ PHE cells. Data are means ± SE of two experiments, each consisting of six replicates.

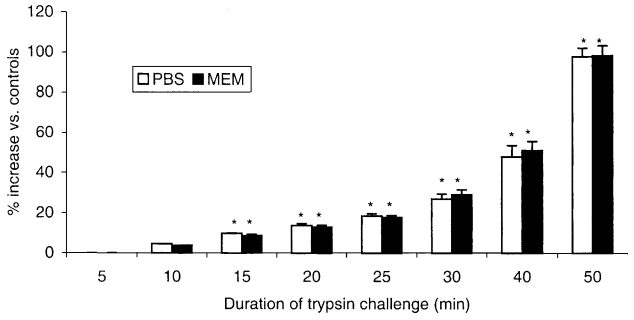

Fig. 2. Optimisation of trypsin exposure time. KB cells, sown on 96-well plastic plates 5 days before, were exposed for 60 min at 0.1 mM NAMI-A in minimum essential medium (MEM) (open bar) or physiological saline (PBS) (black bar). The medium in each well was then replaced with 25 μl of trypsin for different times (5–50 min). Increase in adhesion was evaluated as described in the text. Data are means ± SE of two experiments, each consisting of six replicates. *$P < 0.05$; **$P < 0.01$; Student's unpaired t test.

possible damage to cell integrity. KB cells, challenged with 0.001–0.1 mM NAMI-A for 60 min showed a similar increase of adherent cells vs. untreated controls by 20%, independently of whether the test was done in PBS or MEM; in the same experimental conditions, 0.0001 mM NAMI-A resulted completely inactive (Table 1). Subsequent tests were run with NAMI-A at 0.001–0.1 mM in order to evaluate the concentration effective on cell adhesion (0.001 mM) and that effective on the cell cycle (0.1 mM).

KB tumour cells, challenged with 0.001 and 0.1 mM NAMI-A for 60 min at 0–4 °C or at 37 °C, showed an increase in adherent cells (vs. untreated controls) of about 30% and 20% for cells incubated with MEM or with PBS, respectively (Table 2).

Table 1
Dependence of cell adherence on NAMI-A concentration

NAMI-A concentration (mM)	% increase vs. controls	
	MEM	PBS
0.0001	0.00 ± 0.00	0.00 ± 0.00
0.001	21.30 ± 0.41**	16.50 ± 1.32**
0.01	21.70 ± 0.68**	18.30 ± 1.28**
0.1	25.00 ± 0.61**	21.00 ± 2.01**

MEM, minimum essential medium; PBS, physiological saline.

KB cells were seeded on 96-well plastic plates for 5 days, after which they were exposed for 60 min to different NAMI-A concentrations (0.0001–0.1 mM).

Data are means ± SE of two experiments, each consisting of six replicates.

Student's unpaired t test.

** $P < 0.01$ vs. controls.

Exposure of KB tumour cells to 0.001 and 0.1 mM NAMI-A for 5–240 min immediately produced a statistically significant increase in adherent cells (vs. controls) after 5 min, without any further significant increase when the incubation was increased up to 240 min, and independently of the concentration of NAMI-A (Fig. 3).

4.2. Effect of NAMI-A on the adhesion of HeLa cells

The pro-adhesive effect evaluated as resistance to trypsin treatment, which is a bona fide measure of adhesion strength, was not a typical response of KB cells to NAMI-A. When the effect of NAMI-A was tested on HeLa cells, about the same results were found at the same drug concentrations (+38% at 0.01 mM and +97% at 0.1 mM vs. untreated controls) and after a 1-h challenge.

In this case the pro-adhesive effect was also evaluated on fibronectin, collagen type IV and poly-L-lysine-coated plates. In all the conditions tested, HeLa cells treated with NAMI-A showed significantly increased adherence to the substrate as compared to that in the same test performed with untreated control cells. However, cells grown on plates coated with fibronectin and poly-L-lysine showed the maximum effect with respect to cells grown on plastics or on collagen type IV. Overall, collagen type IV was the substrate to which cells stuck best (Fig. 4).

4.3. Effect of NAMI-A on HPMN adhesion

The capacity of NAMI-A to induce KB and HeLa cells to resist the action of trypsin is not limited to cells growing in adherence to the plate substrate, as shown by the study with HPMN isolated from peripheral blood withdrawn from healthy volunteers (Fig. 5). HPMN

Table 2
Dependence of the effect of NAMI-A on adherence on the temperature of cell challenge

NAMI-A concentration (mM)	% increase vs. controls	
	MEM	PBS
Incubation temperature: 37 °C		
0.001	29.64 ± 1.31**	19.64 ± 2.70*
0.1	35.93 ± 5.30**	17.33 ± 2.33*
Incubation temperature: 0–4 °C		
0.001	30.73 ± 2.60**	16.59 ± 3.36*
0.1	34.39 ± 2.48**	20.54 ± 3.42**

MEM, minimum essential medium; PBS, physiological saline.

KB cells were seeded on 96-well plastic plates for 5 days, after which they were exposed for 60 min to two NAMI-A concentrations (0.001 and 0.1 mM) at 0–4 °C and 37 °C.

Data are means ± SE of two experiments, each consisting of six replicates.

Student's unpaired t test.

* $P < 0.05$.

** $P < 0.01$.

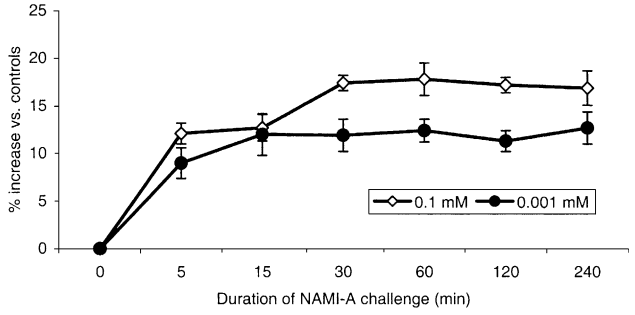

Fig. 3. Effect of NAMI-A on cell adhesion: influence of exposure time. KB cells were sown on 96-well plastic plates 5 days before NAMI-A treatment, then exposed for different times (5–240 min) at two NAMI-A concentrations (0.001 mM, black symbol; 0.1 mM, white symbol). Increase in adhesion was evaluated as described in the text. Data are means ± SE of two experiments, each consisting of six replicates.

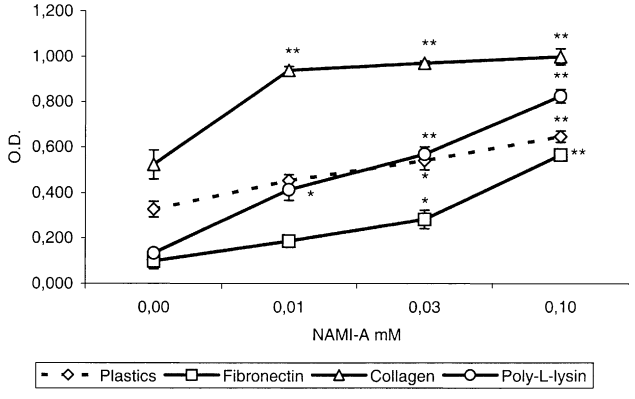

Fig. 4. Effects of NAMI-A on the adhesion of HeLa cells grown on different substrates. HeLa cells, sown on plastics (◇), and on poly-lysine (○), fibronectin (□) or type IV collagen (△), were exposed to 0.1 mM NAMI-A for 60 min. Cell adhesion was determined as described in the text. Data reported are means ± SE of optical density (O.D.) of three different experiments carried out in triplicate. Student's unpaired t test; *$P < 0.05$ and **$P < 0.01$ vs. 0.0 mM NAMI-A.

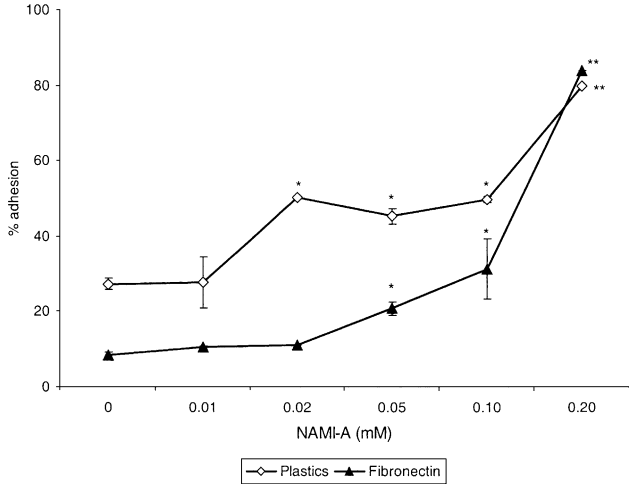

Fig. 5. Effect of NAMI-A on human polymorphonuclear neutrophil adhesion. Neutrophils were sown on plastic (◇) or on fibronectin (FN)-coated surfaces (▲), after 10-min incubation with NAMI-A or in the absence of the drug. The values (data from three different experiments carried out in triplicate) are means ± SE of optical density (O.D.). *$P < 0.05$; **$P < 0.01$; Student's unpaired t test.

exposed in suspension to 10-min challenge with 0.01–0.2 mM NAMI-A showed a statistically significant increase in the number of cells able to stick to the substrate (particularly pronounced at 0.1 and 0.2 mM), taking the number of cells added to the plate as 100%. The effect was evident when either uncoated or fibronectin-coated plates were used. In these conditions, 0.2 mM NAMI-A induced the adhesion of all (100%) of the added cells.

Having shown that NAMI-A increases the adhesion of cells to the substrate and that coating these substrates with proteins of the ECM modulates this adhesion, we investigated the possible involvement of integrins in this NAMI-A-induced effect. To this end we carried out the adhesion assay on HPMN on FN-coated surfaces as described, but in the presence of TS1/18 monoclonal

antibody (20 μg/ml) against the β-chain of β_2-integrins, which are known to be involved in phagocyte adhesion and locomotion. The blocking antibody inhibited the NAMI-A-induced adhesion by about 30%. TNFα-induced adhesion tested in parallel as a positive control was inhibited by 52.4%. Since HPMN express mainly αM β_2-integrin we tested the inhibitory power of monoclonal antibody M1/70 (anti-αM). Blocking the α-chain of this integrin gave the same result, 30.2% inhibition of NAMI-A-induced adhesion (mean of two different experiments), while the blocking monoclonal antibody against αL and integrin gave no significant variation (slight inhibition of 13.7%). These data suggest that the involvement of integrins in the NAMI-A-induced adhesion is conceivable, so we tested if NAMI-A treatment could increase the expression of the activation domain of β_2-integrins on the HPMN surface using monoclonal antibody 24. NAMI-A increased the expression of the activation domain, confirming that β_2-integrins on HPMN surface are activated by NAMI-A and that the effect is comparable to that of TNF used as a positive control (data not shown).

4.4. Morphological appearance of NAMI-A treated cells

Untreated HeLa cells observed by phase-contrast microscopy were mainly round or extending short pseudopodia on either FN- or collagen IV-coated surfaces (see below). Conversely, after NAMI-A treatment, most of them were spread out and extended large pseudopodia, so that they appeared larger than untreated cells. SEM observations confirmed these findings. Untreated cells appeared round, extending small pseudopodia or spread out on the substrate with a polygonal appearance (Fig. 6(a)). After 0.1 mM NAMI-A treatment most of the cells appeared spread out, with large pseudopodial extensions ending with many filopodia (Fig. 6(b)), absent in control cells; no cells with a round appearance were observed. Untreated human neutrophils appeared round despite their interaction with the FN-coated surface (Fig. 6(c)). After treatment with 0.1 mM NAMI-A, they extended a large lamellipodium so thin that it was difficult to obtain good-quality micrographs (Fig. 6(d)).

4.5. NAMI-A effect on actin polymerisation, subcellular distribution and function

NAMI-A, at concentrations active on the pro-adhesive effect, affected the distribution of cellular actin or the extent of its polymerisation either on adherent HeLa cells or on HPMN treated free in suspension. Fig. 7 shows that the subcellular distribution of F-actin, revealed by bound Texas red-conjugated phalloidin, was

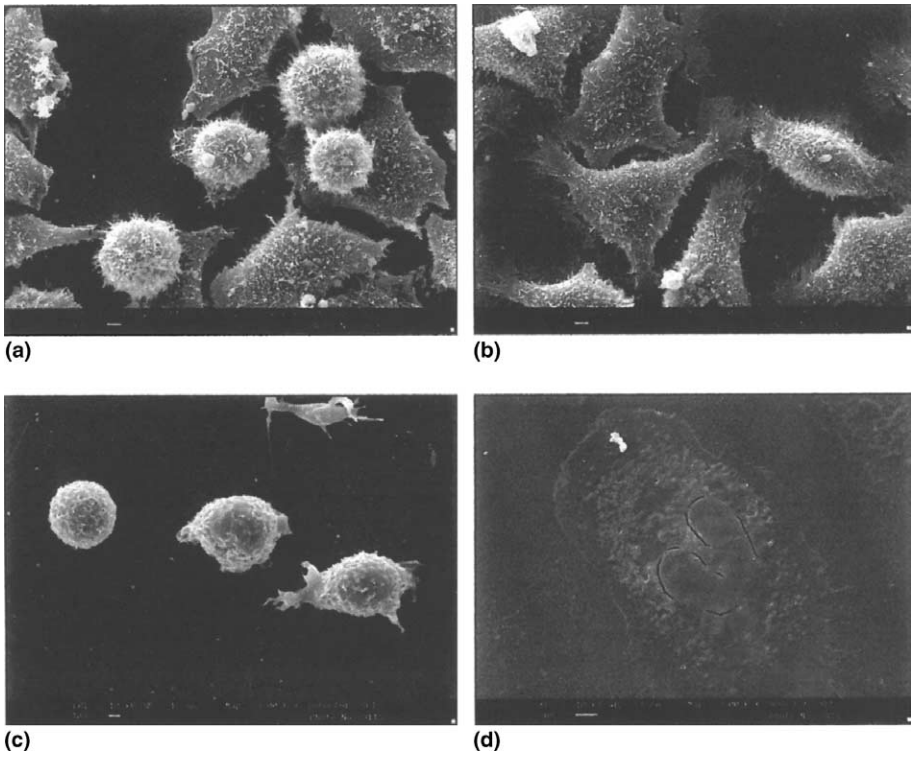

Fig. 6. Scanning electron-microscopic appearance of HeLa cells and human polymorphonuclear neutrophils (HPMN) after NAMI-A treatment. Untreated HeLa cells, final magnification 1750× (a); untreated HPMN, final magnification 2500× (c); NAMI-A-treated (0.1 mM, 60 min) HeLa cells, final magnification 2000× (b); NAMI-A-treated (0.1 mM, 10 min) human HPMN, final magnification 3000× (d).

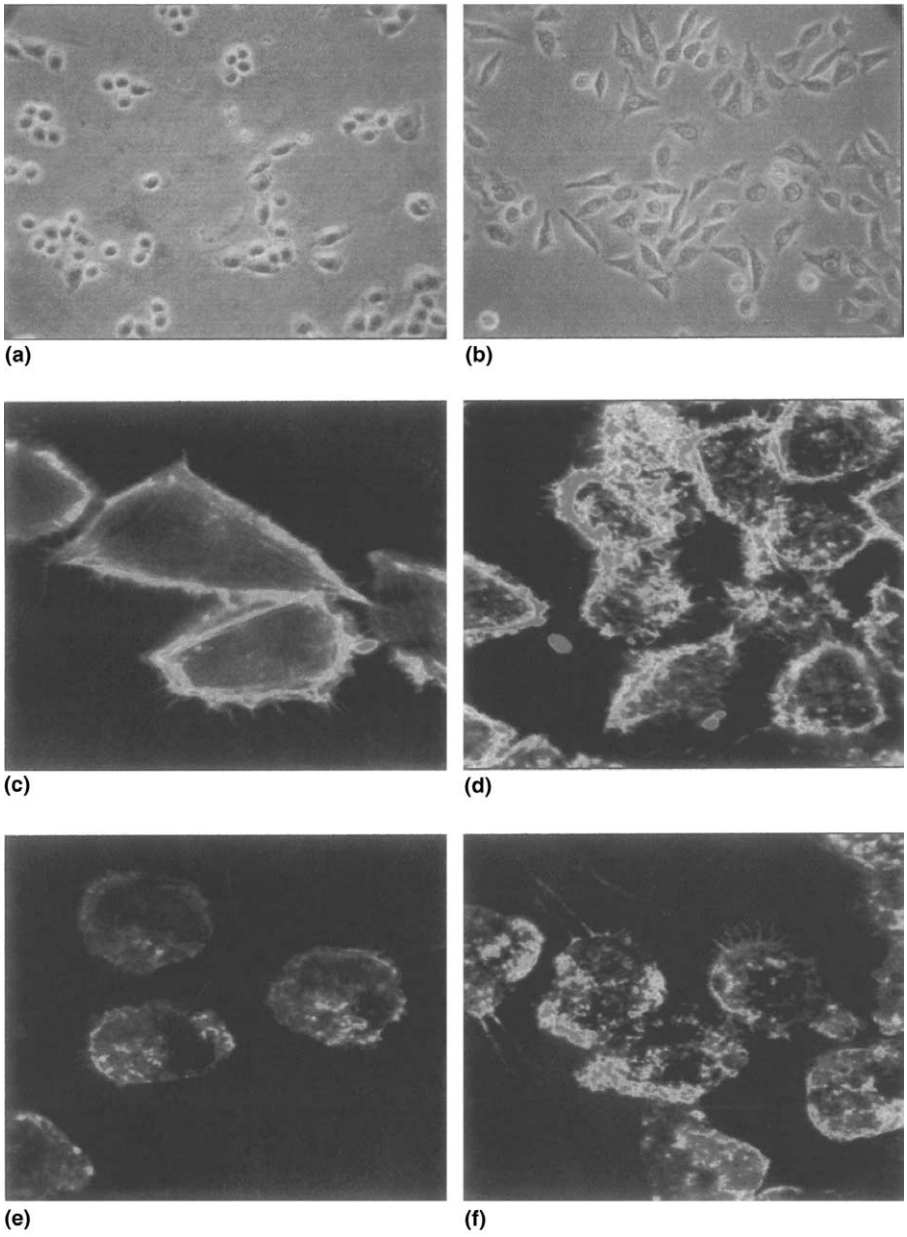

Fig. 7. F-actin distribution in NAMI-A-treated HeLa cells and human polymorphonuclear neutrophils (HPMN) revealed in the confocal microscope by fluorescent phalloidin (pseudo-colour analysis). Untreated HeLa cells (a, c); untreated HPMN (e); NAMI-A-treated (0.1 mM, 60 min) HeLa cells (b, d); NAMI-A-treated (0.1 mM, 10 min) HPMN (f). Original magnification 100×. (a) and (b) are taken from phase-contrast microscopic observations of cells cultured on plastics. Original magnification 40×.

changed after NAMI-A treatment either in HeLa cells (Fig. 7(d)) or on HPMN (Fig. 7(f)), as compared to untreated control cells (Fig. 7(c) and (e), respectively). A small amount of F-actin filaments were found at the edges of control HeLa cells, showing accumulation in defined sites (Fig. 7(c)). Conversely, abundant fibres of F-actin were evident along the entire cell periphery in many NAMI-treated HeLa cells (Fig. 7(d)). These latter appeared smaller than untreated control cells. Since these cells, observed by phase-contrast microscopy, showed the opposite change in shape (Fig. 7(b) vs. (a)), the reduced appearance probably reflects a contraction of actin that leaves filopodia and lamellopodia actin-free. HPMN showed the same changes in F-actin subcellular distribution following exposure to NAMI-A. While untreated control HPMN in suspension show a small amount of F-actin (Fig. 7(e)), the same cells exposed to NAMI-A showed a significant increase of cytosolic F-actin, which appeared to accumulate at one pole of the cell, probably in the correspondence to the site of lamellopodial extrusion (Fig. 7(f)).

The engagement of integrins and of F-actin polymerisation suggested that NAMI-A treatment is able to induce the formation of focal adhesion. So, we investigated

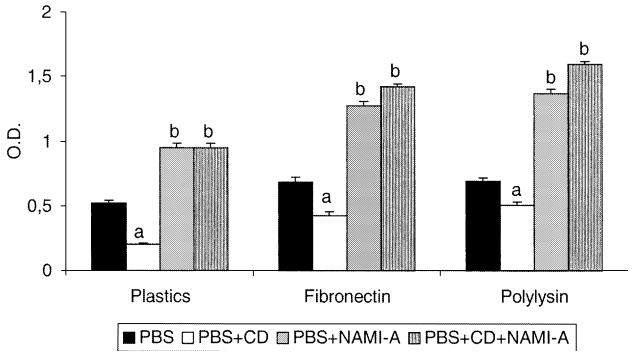

Fig. 8. Effect of cytochalasin D on substrate adhesion of HeLa cells treated with NAMI-A. 1×10^4 HeLa cells were sown on 96-multiwell plates uncoated or coated with fibronectin (FN) from human plasma (50 μl of 20 μg/ml solution) or poly-L-lysine (100 μl of 10 μg/ml solution); 48 h later, two group of cells were pretreated for 5 min with cytochalasin D (5 μg/ml) and one of these groups was subsequently treated for 1 h with 0.010 mM NAMI-A in physiological saline (PBS). A third group of cells was treated only with 0.01 mM NAMI-A in PBS. The adhesion strength was than assayed. Values are means ± SE of optical density (O.D.) readings. Statistical analysis: Student's *t* test; (a) significantly lower than controls (PBS alone) and (b) significantly greater than controls (PBS alone).

if paxillin and Fak, two specific proteins of these structures, were also induced by NAMI-A treatment. The results showed that in NAMI-A-treated HPMN and HeLa cells, neither protein colocalised with actin in focal adhesion, but remained diffused into the cytosol and their signal was too weak to be significant (data not shown).

Data in Fig. 8 show the effects of 0.1 mM NAMI-A on the adhesion of HeLa cells to different substrates, in the presence or in the absence of CD, a well-known actin depolymerising agent. As expected, CD reduced and NAMI-A increased the adhesion of HeLa cells to the substrate. However, CD pretreatment did not modify the effect of NAMI-A when cells were cultured on plastics and even increased the effect of NAMI-A when cells were grown on fibronectin and poly-L-lysine.

The effect of CD on NAMI-A-induced adhesion was also investigated in HPMN. Table 3 shows that the improving effect of NAMI-A on HPMN adhesion was not diminished in the presence of 5 μg/ml CD, rather it was enhanced. The effect of NAMI-A was consistently banished only at the higher CD concentration employed. Even at 20 μg/ml CD, the proportion of trypan blue-positive cells was lower than 5%, which was not significantly different from untreated control cells.

However, despite the failure of 5 μg/ml CD to influence the pro-adhesive effect of NAMI-A, it was shown to interact actively with cells. HPMN treated with NAMI-A in the presence of CD (Fig. 9(b) and (c)) showed a modification of the actin polymerising effect of NAMI-A alone (Fig. 9(a)): at 5 μg/ml CD (Fig. 9(b)) F-actin appeared more diffused while at 20 μg/ml CD it had consistently disappeared from the treated HPMN (Fig. 9(c)).

The ability of NAMI-A to affect cell functions was examined by evaluating phagocytosis of HPMN, a process in which actin is known to play a major part. The Phagocytic Index of untreated HPMN ($PI = 1.6 \pm 0.35$; mean of three experiments) was significantly ($P < 0.05$) increased by 10-min preincubation with NAMI-A before particle addition ($PI = 3.5 \pm 0.4$; mean of three experiments). This increase was ascribed to an increase in HPMN engaged in the ingestion process, from 54% (untreated control cells) to 89% (NAMI-A-treated HPMN).

4.6. Subcellular distribution of NAMI-A in HeLa cells

The subcellular fractionation of NAMI-A-treated HeLa cell homogenate on a sucrose discontinuous gradient allowed the isolation of four distinct fractions, that is, cytosol, membrane, microsomes and nuclei. The highest content of ruthenium (a bona fide measure of NAMI-A binding) per 10^6cells was found in the nuclear fraction (82.6% of the total cell-bound ruthenium) followed by the microsomal (7%), the cytosolic (6.8%) and the membrane fraction (3.6%). However, on a protein basis the ruthenium bound to the membrane fraction was comparable to that found in the nuclear fraction (0.98 ± 0.16 and 1.01 ± 0.13 ng/mg, respectively) and higher than that found in the microsomal (0.47 ± 0.06 ng/mg protein) and in the cytosolic (0.10 ± 0.03 ng/mg

Table 3
Cytochalasin D (CD) effect on NAMI-A-treated human polymorphonuclear neutrophil (HPMN) adhesion

Treatment group	Coated surface	
	Plastics	Fibronectin
NAMI-A	100	100
NAMI-A + 5 mg/ml CD	179	183
NAMI-A + 10 mg/ml CD	76	64
NAMI-A + 20 mg/ml CD	29	25

Each value is the mean of two separate experiments carried out in triplicate; values are expressed as the percentage of adherent cells in the presence of CD, taking the number of adherent HPMN in the presence of NAMI-A as 100%.

The improving effect (relative percentage increment) of NAMI-A was 179% on plastic- and 236% on fibronectin-coated surfaces.

HPMN adhesion was evaluated as reported in Section 2, except that, where indicated, HPMN were incubated for 10 min with CD, NAMI-A, NAMI-A and CD, or in the absence of either compound.

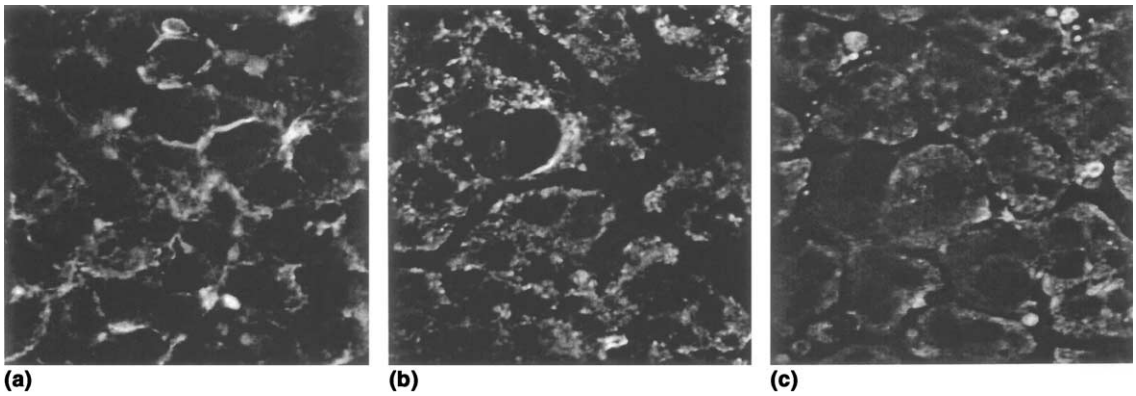

Fig. 9. Effect of cytochalasin D (CD) on actin distribution in HeLa cells treated with NAMI-A. F-actin distribution in NAMI-A-treated human polymorphonuclear neutrophils (HPMN) revealed under the confocal microscope by fluorescent phalloidin. Original magnification 100×. (a) HPMN treated with 0.1 mM NAMI-A for 10 min; (b) HPMN treated with 0.1 mM NAMI-A for 10 min in the presence of 5 μg/ml CD; (c) HPMN treated with 0.1 mM NAMI-A for 10 min in the presence of 20 μg/ml CD.

protein) fractions. Therefore, among the subcellular fractions, apart from the nucleus, the membrane fraction binds significant amounts of NAMI-A.

5. Discussion

NAMI-A increased tumour cell adhesion to the culture substrate at relatively low doses (0.001 mM for KB and 0.01 mM for HeLa cell lines, 0.05 mM for HPMN) already reported to be ineffective on cell-cycle phases (lower limit, 0.1 mM, [5]) or only slightly effective on Matrigel® invasion (0.04–0.12 mM [10,11]), two phenomena that had been associated to the antimetastatic action of NAMI-A on lung metastases of mouse transplantable carcinomas in vivo [9]. The cell-cycle effects of NAMI-A are strictly dependent on its cellular uptake, and the use of a complete culture medium (MEM) or of a low temperature of incubation (0–4 °C) drastically reduces ruthenium uptake and G_2-M arrest [8]. The effect of NAMI-A on cell adhesion seems to be totally independent of the nature of the medium used for cell incubation during the tumour cell challenge (MEM or PBS) and of the temperature used for this challenge (0 or 37 °C). It thus seems that the effects of NAMI-A on cell adhesion are unrelated to the penetration of the compound into cells, or that they are dependent on an effect caused by intracellular concentrations of ruthenium 100-fold lower than those required for other biological effects, including those on the '*ras-myc*' pathway to caspase activation and apoptosis [26,27]. Furthermore, the increase in cell adhesion caused by NAMI-A on KB cells seems to be independent of the concentration of the compound in the range of concentrations used: it is evident at 0.001 mM and remains unaltered with the increasing concentrations up to 0.1 mM.

The pro-adhesive effect of NAMI-A was not a typical response of KB cells to trypsin treatment, since it was also induced in HeLa cells, which, after treatment, assumed a fibroblastic appearance and extruded long and thin filopodia. This behaviour had already been found with TS/A adenocarcinoma cells, typically composed by two subcellular phenotypes, which, after exposure to NAMI-A, showed predominantly the less invasive, fibroblast-like, elongated shape [28].

Even if we cannot exclude that trypsin activity could be inhibited by the drug, the high concentration of enzyme used (500 μg/ml) and the small NAMI-A concentration employed (0.001 mM) were still capable of making the cells non-detachable, making this possibility very unlikely. Conversely, we speculate that the enzyme fails to act because it becomes unable to reach the outer surface of the basal membrane of the adherent cells that interacts with the substrate, due to the strong cell spreading induced by the drug and not because its activity is inhibited. The findings that (i) in other cells (human neutrophils), the pro-adhesive effect of the drug is detectable by a trypsin-independent method, and (ii) that in both tumour cells and neutrophils the actin polymerises after NAMI treatment, support our conclusion and make a study on the effect of NAMI on the proteolytic activity of trypsin less relevant.

The increased pro-adhesive effect induced by NAMI-A was not limited to tumour cells grown in adhesion, since this compound induced a strong pro-adhesive effect also on HPMN treated in suspension. After treatment, HPMN appeared to be completely spread over the substrate, mimicking the morphology observed with HeLa cells.

The morphological changes induced in the treated cells by NAMI-A may well depend on its effect on actin polymerisation. After treatment with NAMI-A, HeLa cells show actin bundles more prominently and probably contracted (they have a smaller diameter) compared to untreated controls. The same increase in F-actin was found in HPMN following NAMI-A addition. The

observations that F-actin increases in HPMN during the adhesion process [29], a phenomenon required for HPMN spreading [30], and that F-actin is required for tumour cell adhesion to substrate [31–33], support the causal relation between actin polymerisation, spreading and adhesion. NAMI-A was also shown to influence actin function in HPMN, as judged by the increased number of HPMN engaged in the ingestion process. Furthermore, NAMI-A was also able to improve significantly the aortic tension induced by PHE, at concentrations active in inducing the pro-adhesive effect (M. Vadori; unpublished data from a Ph.D. study; Department of Biomedical Sciences, University of Trieste), an effect associated with stimulation of microfilament contraction in aortic smooth-muscle cells [34]. Finally, the polymerisation of F-actin promoted by NAMI-A seems insensitive to the effect of cytochalasin D at 5 μg/ml, a finding that suggests that after interaction with NAMI-A, F-actin becomes resistant to the effect of depolymerising factors, further supporting the hypothesis that NAMI-A modifies the function of F-actin.

Why CD at the lowest concentration employed improved the NAMI-A-induced adhesion in HeLa cells and HPMN is not known. Its concentration must be increased up to 20 μg/ml to hinder the pro-adhesive effect of NAMI-A and the induction of F-actin depolymerisation, which supports the hypothesis that F-actin contributes to adhesion. Even if it did not affect cell viability, this concentration of CD is rather high. Its effect on HPMN had already begun at 5 μg/ml, but failed to hinder the (either direct or indirect) interaction of NAMI-A with the cell target. Both the improving effect of CD on adhesion and the resistance to depolymerisation of F-actin in NAMI-A-treated cells are findings that deserve a deeper investigation at the molecular level.

After exposing HeLa cells to 0.3 mM NAMI-A, ruthenium rapidly entered the intracellular environment. The evaluation of the extent of ruthenium's subcellular distribution on a protein basis showed that the compound (or its metabolites) associates, after 15-min incubation, mainly with the membrane and the nuclear fraction, while its concentration was significantly lower in both the microsomal and cytosolic fraction. On this basis we speculate that the effect on cell adherence might depend on the action of NAMI-A at the membrane level, a site where F-actin is known to interact [35,36], rather than to effects on other intracellular targets. This hypothesis is supported by:

1. The rapid onset of this effect after the exposure of KB cells to NAMI-A; the increase in cell adhesion reached its maximum a few minutes after cell challenge without any further increase in the subsequent 240 min.
2. The dissociation from NAMI-A's pro-adhesive effect and NAMI-A's uptake, which requires 37 °C.

The mechanism underlying the pro-adhesive effect of NAMI-A is unknown, but the observation that the compound is active in this sense also when cells are kept at low temperature (4 °C) is suggestive of a chemical interaction with a membrane target.

That NAMI-A is found in a bound form at the HeLa cell membrane suggests that at this site the drug can act by modulating integrin activation, actin-binding protein activation and actin polymerisation. The higher amount found in the nucleus can explain the effect induced by NAMI-A on the cell cycle, which, however, is observed at concentrations higher than those inducing pro-adhesive effects. It is noteworthy that NAMI-A has anti-metastatic effects at concentrations lower than those required for affecting the cell cycle. Recently, we reported that the presence of serum or a low temperature of incubation inhibits NAMI-A uptake by the treated cells. The residual cell-associated NAMI-A is very probably accounted for by that amount which is bound to the cell membrane. We think it likely that while the uptake of the compound into the cell (cytosol, microsomes and nucleus) requires energy and is revealed at its maximum value in PBS and at 37 °C, the membrane-bound NAMI-A is largely independent of energy production. We did not further investigate this problem but we speculate that this is the reason why the pro-adhesive effect of NAMI-A is not affected by the presence of MEM, temperature or PBS: it is induced by the amount of membrane-bound NAMI-A, which we believe is independent of cellular uptake.

The mechanism of the pro-adhesive effect of NAMI-A merits further investigation, and the increased activation of integrins is only one possible event. Our data suggest that the involvement of integrins cannot account completely for this effect: first, the inhibition induced by β- and α-chain-blocking antibodies is not complete, and secondly, NAMI-A also increases the adhesion of cells on poly-L-lysine-coated surfaces, where integrins are not involved. Therefore the effect of NAMI-A could be more complex and it might involve more than one mechanism, or conversely it might activate a more central mechanism capable of inducing adhesion both through integrin activation and through other mechanisms, such as a direct effect on actin polymerisation. However, even if our findings argue for an integrin engagement together with a stimulus to F-actin polymerisation in NAMI-A-treated human HPMN, these appear incapable of organising focal adhesions. In fact, we could not find any focal signal when the subcellular distribution of paxillin and Fak, two focal adhesion proteins, was investigated.

Globally, the effects of NAMI-A on cell adhesion, as well as the reported effects on invasion [9], on angiogenesis [10], on ERK1/2 inhibition [26] and on caspase activation [27], throw new light on the mechanism of metastasis reduction. Adhesion and invasion are two

steps in the same process that leads, as an endpoint, to metastasis formation [1,2], and NAMI-A is a potent inhibitor of metastasis formation and growth [11].

As far as the reduction of metastatic potential is concerned, we envisage the following. NAMI-A rapidly interacts, with one or more targets at the membrane level, where it triggers integrin activation, actin nucleation and microfilament elongation, a process known to be related causally to adhesion in phagocytes [29] and tumour cells [32,33]. Accordingly, treated cells strongly interact with the substrate through actin fibres. These fibres may be resistant to depolymerising stimuli, as judged by their CD resistance, and primed to contract, perhaps after interaction with myosin, making the cells irreversibly and strongly linked to the substrate, and hence immobile. The final outcome is a strong inhibition of cell migration that requires continuous cycles of actin polymerisation/depolymerisation. We think that this inhibition of cell migration, already reported elsewhere as an effect of NAMI-A [9,10], is at least one of the mechanisms underlying the inhibition of the metastatic process (spread and growth) induced by this compound.

In conclusion, our findings on the effects of NAMI-A indicate that this drug can strongly modify the structure of the actin cytoskeleton, affect the function of integrins, and the adhesion of HPMN and HeLa cells to substrates. These processes are related to cell locomotion and hence tumour invasiveness.

Acknowledgements

Work contributed by MIUR (ex-40% 'Pharmacological mechanisms of the antimetastatic activity of metal-based drugs') and from LINFA – Callerio Foundation Onlus; the work was done in the frame of COST D20/0005/01. The authors thank Marta Cervi for her skilful technical assistance.

References

1. Thompson EW, Price JT. Mechanisms of tumour invasion and metastasis: emerging targets for therapy. *Expert Opin Ther Targets* 2002, **6**, 217–233.
2. Bashyam MD. Understanding cancer metastasis. *Cancer* 2002, **94**, 1821–1829.
3. Brakebusch C, Bouvard D, Stanchi F, Sakai T, Fässler R. Integrin in invasive growth. *J Clin Invest* 2002, **109**, 999–1006.
4. Tsuij T, Kawada Y, Kai-Murozono M, Komatsu S, Han SA, Tacheuchi K, *et al*. Regulation of melanoma cell migration and invasion by laminin-5 and $\alpha 3\beta 1$ integrin (VLA-3). *Clin Expl Metastasis* 2002, **19**, 127–134.
5. Bergamo A, Gagliardi R, Scarcia V, Furlani A, Alessio E, Mestroni G, *et al*. In vitro cell cycle arrest, in vivo action on solid metastasizing tumours, and host toxicity of the antimetastatic drug NAMI-A and cisplatin. *J Pharmacol Expl Ther* 1998, **289**, 559–564.
6. Sava G, Clerici K, Capozzi I, Cocchietto M, Gagliardi R, Alessio E, *et al*. Reduction of lung metastasis by ImH[trans-$RuCl_4$(DMSO)Im]: mechanism of the selective action investigated on mouse tumours. *Anticancer Drugs* 1999, **10**, 129–138.
7. Bergamo A, Zorzet S, Cocchietto M, Carotenuto ME, Magnarin M, Sava G. Tumour cell uptake G2-M accumulation and cytotoxicity of NAMI-A on TS/A adenocarcinoma cells. *Anticancer Res* 2001, **21**, 1893–1898.
8. Frausin F, Cocchietto M, Bergamo A, Scarcia V, Furlani A, Sava G. Tumour cell uptake of the metastasis inhibitor ruthenium complex NAMI-A and in vitro effects on KB cells. *Cancer Chemother Pharmacol* 2002, **50**, 405–411.
9. Zorzet S, Bergamo A, Cocchietto M, Sorc A, Gava B, Alessio E, *et al*. Lack of in vitro cytotoxicity, associated to increased G_2-M cell fraction and inhibition of matrigel invasion, may predict In vivo-selective antimetastasis activity of ruthenium complexes. *J Pharmacol Expl Ther* 2000, **295**, 927–933.
10. Vacca A, Bruno M, Boccarelli A, Coluccia M, Ribatti D, Bergamo A, Garbisa S, *et al*. Inhibition of endothelial cell functions and of angiogenesis by the metastasis inhibitor NAMI-A. *Br J Cancer* 2002, **86**, 993–998.
11. Sava G, Zorzet S, Turrin C, Vita F, Soranzo MR, Zabucchi G, *et al*. Dual action of NAMI-A in inhibition of solid tumour metastasis: selective targeting of metastatic cells and binding to collagen. *Clin Cancer Res* 2003, 1898–1905.
12. Craciunescu DG, Scarcia V, Furlani A, Doadrio A, Ghirvu C, Ravalico L. Cytostatic and antitumour properties of a new series of Pt (II) complexes with cyclopentylamine. *In vivo* 1987, **1**, 229–234.
13. Eagle H. Amino acid metabolism in mammalian cell cultures. *Sciences* 1959, **130**, 432–437.
14. Marzano C, Severin E, Pani B, Guiotto A, Bordin F. DNA damage and cytotoxicity induced in mammalian cells by a tetramethylfluroquinolinone derivative. *Environ Mol Mutagen* 1997, **29**, 256–264.
15. Skehan P, Storeng R, Scudiero D, Monks A, McMahon J, Vistica D, *et al*. New colorimetric cytotoxicity assay for anticancer-drug screening. *J Natl Cancer Inst* 1990, **82**, 1107–1112.
16. Menegazzi R, Busetto S, Dri P, Cramer R, Patriarca P. Chloride ion efflux regulates adherence, spreading, and respiratory burst of neutrophils stimulated by tumour necrosis factor-alpha (TNF) on biologic surfaces. *J Cell Biol* 1996, **135**, 511–522.
17. Menegazzi R, Zabucchi G, Knowles A, Cramer R, Patriarca P. A new, one-step assay on whole cell suspensions for peroxidase secretion by human neutrophils and eosinophils. *J Leukoc Biol* 1992, **52**, 619–624.
18. Sanchez-Madrid F, Krensky AM, Ware CF, Robbins E, Strominger JL, Burakoff SJ, *et al*. Three distinct antigens associated with human T-lymphocyte-mediated cytolysis: LFA-1, LFA-2 and LFA-3. *Proc Natl Acad Sci USA* 1982, **79**, 7489–7493.
19. Huang C, Springer TA. Folding of the beta-propeller domain of the integrin alphaL subunit is independent of the I domain and dependent of the beta2 subunit. *Proc Natl Acad Sci USA* 1997, **94**, 3162–3167.
20. Thornton BP, Vetvicka V, Pitman M, Goldman RC, Ross GD. Analysis of the sugar specificity and molecular location of the β-glucan-binding lectin site of complement receptor type 3 (CD11b/CD18). *J Immunol* 1996, **156**, 1235–1246.
21. Herzog M, Draegar A, Ehler E, Small JV. Immunophluorescence microscopy of the cytoskeleton. In *Cell biology laboratory handbook*, 2nd ed. vol. 2, 1994, 355–360.
22. Benedetti A, Fulceri R, Comporti M. Calcium sequestration activity in rat liver microsomes. Evidence for a cooperation of calcium transport with glucose-6-phosphatase. *Biochim Biophys Acta* 1985, **816**, 267–277.
23. Bergmayer HU. In: *Method of enzymatic analysis*, vol. 2. EDS, Bergmeyer and Grassel, 1983.

24. Tamura H, Arai T. Determination of ruthenium in biological tissue by graphite furnace AAS after decomposition of the sample by tetramethylammonium hydroxide. *Bunseki Kagaku* 1992, **41**, 13–17.
25. Tallarida RJ, Murray RB. Manual of pharmacological calculation with computer programs. 2nd ed. New York, Springer, 1986.
26. Sanna B, Debidda M, Pintus G, Tadolini B, Posadino AM, Bennardini F, *et al*. The antimetastatic agent imidazolium trans-imidazoletetrachloro-ruthenate induces endothelial cell apoptosis by inhibiting the mitogen-activated protein kinase/extracellular signal-regulated kinase signaling pathway. *Arch Biochem Biophys* 2002, **403**, 209–218.
27. Pintus G, Tadolini B, Posadino AM, Sanna B, Debidda M, Bennardini F, *et al*. Inhibition of the MEK/ERK signaling pathway by the novel antimetastatic agent NAMI-A down regulates c-myc gene expression and endothelial cell proliferation. *Eur J Biochem* 2002, **269**, 5861–5870.
28. Pacor S, Magnarin M, Carotenuto ME, Spessotto P, Zabucchi G, Sava G. In vitro growth of TS/A adenocarcinoma and of the gene transfected TS/A-IL4 line on biological substrates. *Anticancer Res* 2000, **20**, 191–196.
29. Southwick FS, Dabiri GA, Paschetto M, Zigmond SH. Polymorphonuclear leucocyte adherence induces actin polymerization by a transduction pathway which differs from that used by chemoattractants. *J Cell Biol* 1989, **109**(Pt 1), 1561–1569.
30. Galkina SI, Sud'ina GF, Ullrich V. Inhibition of neutrophil spreading during adhesion to fibronectin reveals formation of long tubulovesicular cell extensions (cytonemes). *Exp Cell Res* 2001, **266**, 222–228.
31. Haier J, Nasralla M, Nicolson GL. Different adhesion properties of highly and poorly metastatic HT-29 colon carcinoma cells with extracellular matrix components: role of integrin expression and cytoskeletal components. *Br J Cancer* 1999, **80**, 1867–1874.
32. Haier J, Nicolson GL. Role of the cytoskeleton in adhesion stabilization of human colorectal carcinoma cells to extracellular matrix components under dynamic conditions of laminar flow. *Clin Exp Metastasis* 1999, **17**, 713–721.
33. Suzuki K, Takahashi K. Actin filament assembly and actin-myosin contractility are necessary for anchorage- and EGF-dependent activation of phospholipase Cgamma. *J Cell Physiol* 2001, **189**, 64–71.
34. Garay RP. Cellular mechanisms of smooth muscle contraction. *Rev Mal Respir* 2000, **2 Pt 2**, 531–533.
35. Greenberg S, Grinstein S. Phagocytosis and innate immunity. *Curr Opin Immunol* 2002, **14**, 136–145.
36. Hartwig JH, Thelen M, Rosen A, Janmey PA, Nairn AC, Aderem A. MARCKS is an actin filament crosslinking protein regulated by protein kinase C and calcium–calmodulin. *Nature* 1992, **356**, 618–622.